The 2013 World Congress on
Advances in Structural Engineering and Mechanics (ASEM13)
Jeju, Korea, September 8-12, 2013

Numerical simulation of rock berm under anchor collision

*Jinho Woo[1)], Won-Bae Na[2)] and Jeong-Seok Yu[3)]

[1), 2)] *Department of Ocean Engineering, Pukyong National University, Busan 608-737, Korea*
[3)] *Korea Ocean Engineering & Consultant Co., Ltd., Suwon 442-190, Korea*
[2)] *wna@pknu.ac.kr*

ABSTRACT

Rock berm is frequently used for protection of underwater lifelines such as pipelines and power cables. During the service life, rock berm can experience several accidental loads such as anchor collision. The consequences can be severe with a certain level of frequency; hence, the structural responses should be carefully understood. However, no study has been made to quantify the structural responses because it is hard to deal with the individual behavior of each rock. Therefore, this study presents a collision analysis of rock berm using a finite element software, ANSYS AUTODYN, by facilitating the smoothed-particle hydrodynamics method. The analysis results were compared with the those obtained from the Lagrange method. Moreover, two different drop velocities (2.747 and 5 m/s) were selected to investigate the changes in the responses. Finally, the effect of these parameters (analysis method and drop velocity) on the analysis results was studied; accordingly, the relation between the parameters and damages were found.

1. INTRODUCTION

Rock has been used as common construction material, particularly for constructing protective structures such as the embankments and berms. Rock berm has been used to protect underwater lifelines such as pipelines and power cables from hydrodynamic forces due to currents and accidental dynamic loadings due to anchor impact and drag. Many studies have explored for a rock berm. Most studies focused on stability of berm breakwaters (Corkum and Martin 2004; Tørum et al. 2012). Also, numerical analysis of rock material concentrated on the fracture of rock under explosion and high strain rate loading (Hao and Hao 2013; Zhu et al. 2007). However, response of rock berm under low speed impact is a deviation from the studies above.

[1)] Graduate Student
[2)] Professor
[3)] Doctor of Engineering

This study concerns of low velocity impact on rock berm, for the purpose of protecting submarine pipelines and power cables under more challenging, unpredictable threats. For the analysis, a transient finite element dynamic analysis was carried out to capture the dynamic response of rock berm particularly by facilitating the smoothed-particle hydrodynamics (SPH) method, which can simulate the individual behavior of each rock. By comparing the analysis results with those obtained from the typical analysis method, so-called Lagrange, the applicability of the newly adopted SPH is discussed. In addition, the anchor drop height is intentionally varied from 2.747 m/s to 5 m/s to capture how the change in drop height affects the structural response. It should be noted here that the general purpose finite element software, ANSYS AUTODYN, is used for the analyses.

2. FEM Modeling

This work employs an explicit finite element method program ANSYS AUTODYN. A four-node shell element is used to model the rigid anchor as shown in Fig. 1. Material properties of the anchor are shown in Table 1 and modeling of the anchor is made according to the KS V 3311 (2012). Rock berm modeling was carried out by two parts; bottom sand, and rock. Material properties of the materials are shown in Table 1 (Gere 2004). Bottom sand was modeled as the linear elastic material. The impact point is located at the center as shown in Fig. 2. For collision analysis, two impact velocities (2.747 and 5 m/s) of the anchor were considered. Here, the terminal velocity of the anchor is known 2.747 m/s by carefully considering the drag coefficient of the anchor (Woo and Na 2013). To determine the effect of impact velocity, an additional velocity 5 m/s was considered. The interval between the anchor and rock berm is fixed to 20 mm. In the simulation, the vertical displacement of the bottom sand was constrained and the horizontal displacement of the rock berm was also constrained.

Fig. 1 Shape of anchor modeling

Table 1 The properties of materials

	Density (kg/m3)	Young's modulus	Poisson ratio
Anchor	7200	170 GPa	0.25
Bottom sand	2200	81 MPa	0.3

SPH and Lagrange method were used to model the rock berm and the dimensions are shown in Fig. 2. The lower and upper widths are 11.1m and 2.5m, respectively. The height is 2.1m. Since the material model is quite significant for the impact simulation, the rock material is composed the three equations: linear equation of state, piece-wise Drucker-Prager strength criterion, and tensile failure condition. Piece-wise Drucker-Prager strength criterion includes strength and failure model. This model represents the pressure-yield behavior of the rock with a piece-wise linear function, constructed using several pressure-yield points. Fig. 3 show pressure-yield stress curve. The rock material properties are given in Table 3 (Chen et al. 2000).

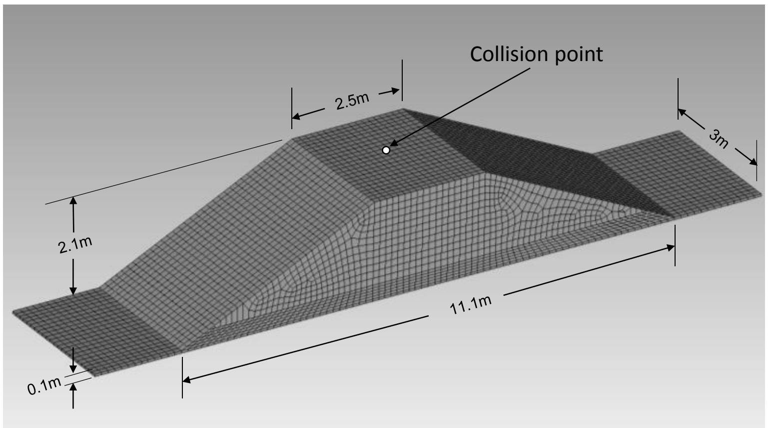

Fig. 2 Rock berm modeling

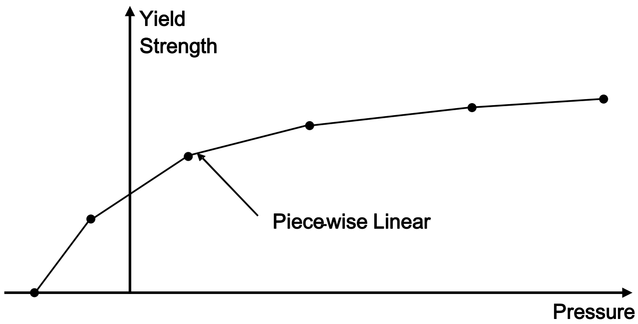

Fig. 3 Piece-wise pressure-yield stress curve

Table 2 The material properties of rock

Parameter	Value	Parameter	Value
Density (kg/m^3)	2750	Shear modulus (GPa)	17.44
Bulk modulus (GPa)	35.7	Hydro tensile limit (MPa)	30
Pressure 1 (MPa)	-30	Yield stress 1 (MPa)	0
Pressure 2 (MPa)	-26.7	Yield stress 2 (MPa)	40
Pressure 3 (MPa)	200	Yield stress 3 (MPa)	450
Pressure 4 (MPa)	1000	Yield stress 4 (MPa)	1430
Pressure 5 (MPa)	2500	Yield stress 5 (MPa)	2530

3. Analysis method

As described above, SPH and Lagrange methods were used to model the rock berm. The Lagrange method is mainly used for structural finite element analysis. The features of Lagrange method are as follows: nodes move and with the material and normally used for modelling of solid continua in the simulation. Therefore, the Lagrange method isn't suitable for analysis of discontinuous material just like sand, rock, and fluid.

SPH method is a gridless (meshless) technique. The main advantage of this method is to bypass the requirement for a numerical grid to calculate spatial derivatives. This avoids the severe problems associated with mesh tangling and distortion which usually occur in Lagrangian analyses involving large deformation impact loading events. In the SPH method, basic steps used in each calculation cycle, are shown in Fig. 4. The SPH method uses kernel approximation, which is based on randomly distributed interpolation points with no assumptions about which points are neighbors, to calculate spatial derivatives (Hayhurst 1996).

SPH particle was used in the rock berm section. In the SPH method, particle size is a very important factor because an accuracy of the result depends on the number of particles which are used in unit volume (Sakakibara 2008). In the FEM simulation, particle size is 200mm the same as the average diameter of rock. The interaction between particles was considered, but the coupling between particles is not considered like a real rock.

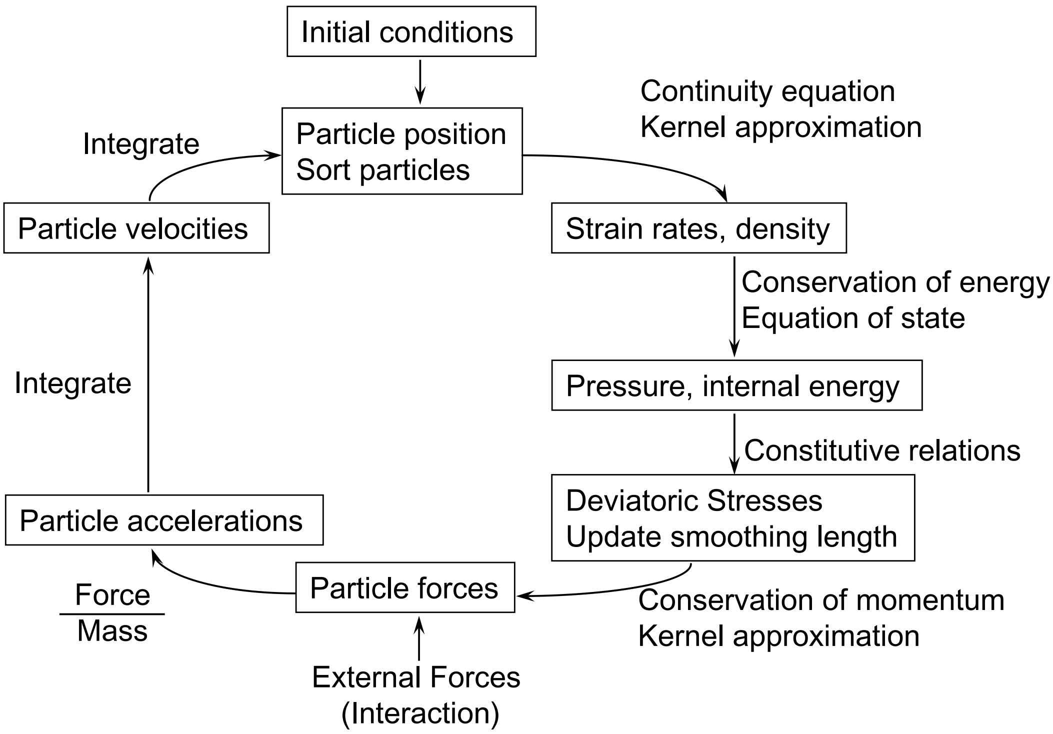

Fig. 4 Computational cycle for SPH method

4. Results

Depending on the analysis method and collision velocity, anchor collision simulations are performed for each case shown in Table 3. Fig. 5 (a) is the von-Mises stress distribution of Lagrange model. Fig. 5 (b) is the von-Mises stress distribution in cross-section of SPH model.

In Fig. 5 (a) showing the analysis result of Case 1, the von-Mises stress is concentrated on the collision region. Fig. 5 (b) is the von-Mises stress distribution in cross-section of Case 3. In this figure, the direction and length of arrow indicate the stress direction and size of von-Mises stress. The stress is concentrated on the collision region, and the stress spreads to the circumference region. From the figures, it is hard to compare the stress distributions. Therefore, five gauge points were selected to get the response of the simulation. The first point is the collision point and consecutive points were selected with vertical intervals of 500mm from the first point, respectively.

Fig. 6 shows von-Mises stress of each gauge point in the cases of 1 and 2. It is shown from Fig. 6 that stress distributions are similar and von-Mises stress becomes bigger when the collision velocity increases. Fig. 7 shows von-Mises stress of each gauge point in the cases of 3 and 4. It is shown from Fig. 7 that stress distributions are also similar and von-Mises stress becomes larger when the collision velocity increases. It is shown from all of the results that stress at point 1 is bigger than other gauge points, as expected. By comparing the Lagrange method with SPH method, it is shown that von-Mises stresses are different in the ways of magnitude and pattern.

Table 3 Simulation cases

	Analysis method	Collision velocity
Case 1	Lagrange	2.747 m/s
Case 2	Lagrange	5 m/s
Case 3	SPH	2.747 m/s
Case 4	SPH	5 m/s

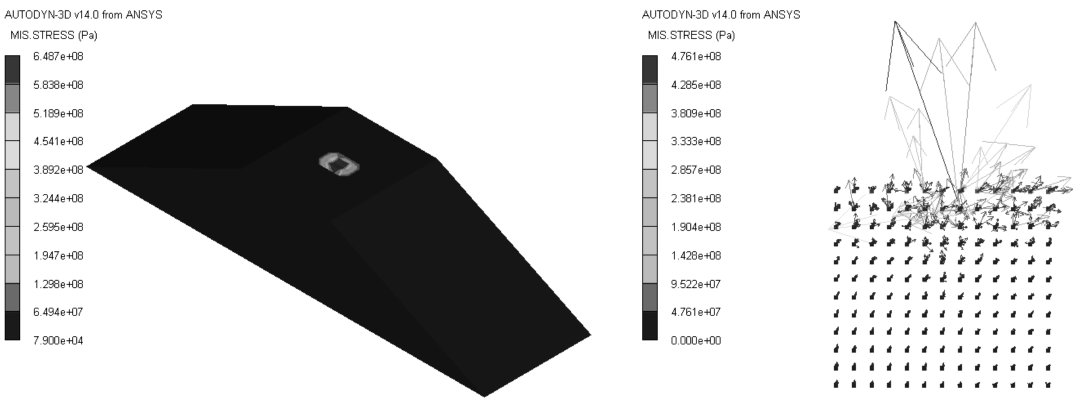

(a) Case 1 (b) case 3

Fig. 5 Von-Mises stress contours of Case 1 and Case 3

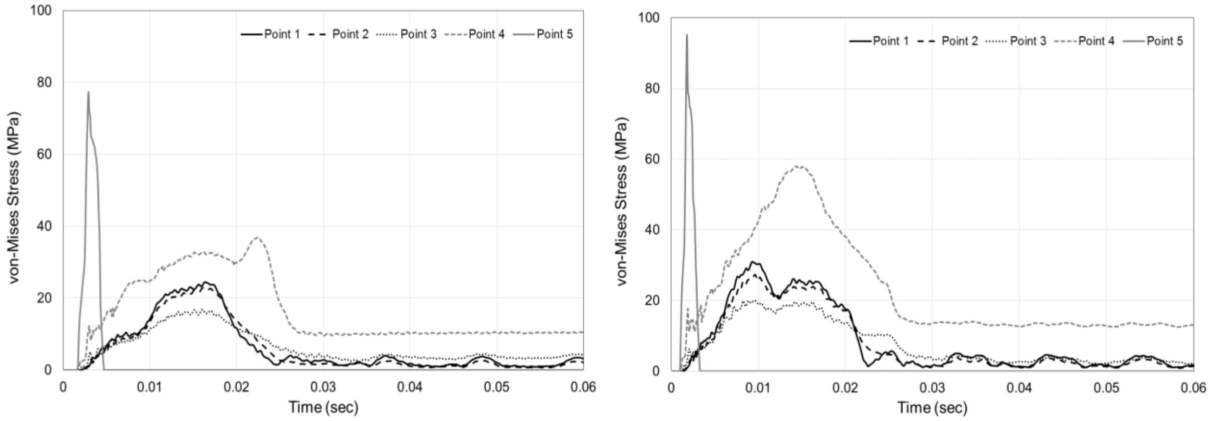

(a) Case 1 (b) Case 2

Fig. 6 von-Mises stress of case 1 and 2

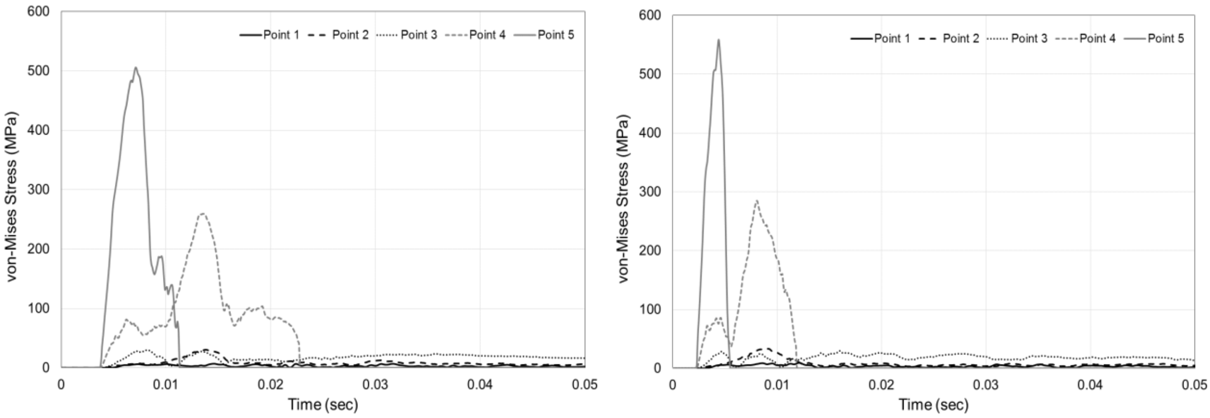

(a) Case 3 (b) Case 4

Fig. 7 von-Mises stress of case 3 and 4

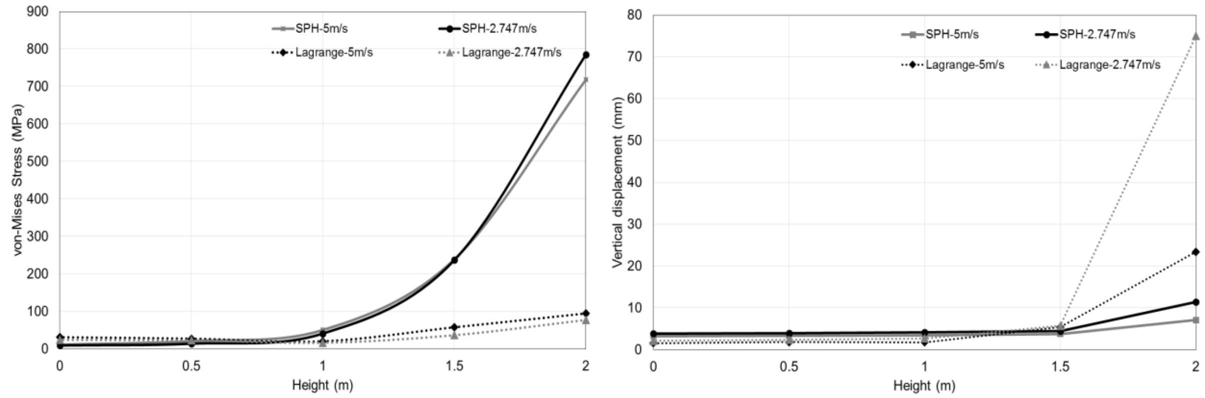

(a) Maximum von-Mises stress (b) Vertical displacement

Fig. 8 The response of each gauge point

Fig. 8 (a) and Table 4 show the maximum von-Mises stress of each point denoted by Point 1 (2m), Point 2 (1.5m), Point 3 (1m), Point 4 (0.5m), and Point 5 (0m). The maximum stresses are similar within each analysis method. As discussed, the stress values recorded in Lagrange method were lower than the values recorded in SPH. In most of the results, the maximum stress decreases as distance from the collision point (gauge 1) increases. An interesting fact in the cases of 1 and 2 is that stresses at points 4 and 5 are bigger than the stresses at point 3. This is obviously not expected but explainable because of the nature of Lagrange method – each element connected by a shared node unlike SPH. In other words, the coupling between elements and interaction with the bottom boundary conditions cause the fact. In contrast, the results of SPH, cases 3 and 4, show the stresses become smaller as the gauge point is bigger, as expected. Besides, these stresses are much larger than those of cases 1 and 2 because the nature of SPH – the interaction between particles.

Fig. 8 (b) and Table 5 show the vertical displacement of each gauge point. In all of the results, the vertical displacement decreases as distance from collision point increases. The results of points 1 and 2 show that the displacements obtained from Lagrange method is larger than those obtained from SPH. However, the results of points 3, 4, and 5 show the opposite way.

Table 4 Maximum Von-Mises stress of each gauge point

	Case 1	Case 2	Case 3	Case 4
Point 1 (2m)	77.3	95.2	718	785
Point 2 (1.5m)	36.8	57.9	239	237
Point 3 (1m)	16.8	20.0	50.4	41
Point 4 (0.5m)	22.9	27.2	20.9	14
Point 5 (0m)	24.5	31.0	11.3	9.42

Table 5 Maximum vertical displacement of each gauge point

	Case 1	Case 2	Case 3	Case 4
Point 1 (2m)	23.4	75.0	7.09	11.4
Point 2 (1.5m)	5.42	5.71	3.75	4.49
Point 3 (1m)	1.77	2.70	3.48	4.14
Point 4 (0.5m)	1.81	2.41	3.36	3.98
Point 5 (0m)	1.59	2.12	3.26	3.86

It should be noted here that the structural properties of submarine cables on the existing research are hard to find. Most studies focused on electronic analyses of underwater power cable (Zhang et al. 2013; Kalcon et al. 2013). Thus, the stability of underwater power cable was examined using not compressive strength but the tensile and flexural strength. According to a study by Tanaka and Kunii (2000), tensile strength of the modified HDPE cable is 27MPa, and the bending strength is 37MPa. From the results of von-Mises stress, the stresses of gauges 4 and 5 satisfy the criteria. This means that the underwater power cable is safe from anchor collision when the height of the rock berm is over 1.5m. It should be noted here that this observation is assumed only if stress of rock is spread completely to power cable.

5. CONCLUSIONS

This paper represents the transient dynamic analyses of rock berm under anchor collision. Two analysis methods (Lagrange and SPH) and two collision velocities (2.747 m/s, and 5 m/s) are considered in the analyses. The responses of rock berm were measured at five different gauge points. The influences of the analysis method and the collision velocity were investigated. From the collision analyses, the following conclusions are drawn. (1) In stress analysis, SPH produces larger values near the impact point but the deviation becomes smaller far from the impact. Lagrange method is not proper to quantify the stresses near the bottom because it does describe improper stress patterns near the bottom. (2) In displacement analysis, SPH produces smaller values near the impact point but the deviation becomes smaller far from the impact. From the study, it is shown that SPH method is the one we should use in the transient dynamic analyses of rock berm under anchor collision.

Acknolwedgement

This research was a part of the project titled “Development on the Guidelines of Safety Assessment for Submarine Cable Protection Facilities in Shallow Water” funded by the Ministry of Land, Transport and Maritime Affairs, Korea (KIMT – 2012 – 20120018).

REFERENCES

Chen, S.G., Zhao, J., Makurati, A. and Madshus, C. (2000), Discrete element modelling of an explosion test in granite, *Proceedings of GeoENG2000 International Conference on Geotechnical, Geological Engineering*, Melbourne.

Corkum, A.G. and Martin, C.D. (2004), Analysis of a rock slide stabilized with a toe-berm: a case study in British Columbia Canada, *Int. J. Rock Mechanics & Mining Science*, Vol. 41, 1109-1121.

Gere, J.M. (2004), *Mechanics of Materials*, Thomson, Belmont, CA.

Hao, Y. and Hao, H. (2013), Numerical Investigation of the Dynamic Compressive Behaviour of Rock Materials at High Strain Rate, *Rock Mech. & Rock Eng.*, Vol. 46, 373-388.

Hayhurst, C.J., Clegg, R.A., Livingstone, I.H. and Francis, N.J. (1996), The Application of SPH Techniques in AUTODYN-2D to Ballistic Impact Problems, *Proceeding of 16th International Symposium on Ballistics*, San Francisco.

Kalcon, G., Adam, G.P., Anaya-Lara, O. and Lo, K.L. (2013), Analytical efficiency evaluation of two and three level VSC-HVDC transmission links, *International Journal of Electrical Power & Energy Systems*, Vol. 44, 1-6.

KS V 3311 (2012) Anchors, Korean Standard.

Sakakibara, T., Tsuda, T. and Ohtagaki, R. (2008), A Study of Quasi-static Problem by SPH Method, *10th international LS-DYNA users conference*, Dearborn.

Tanaka, T. and Kunii, K. (2000), High Performance HVDC Polymer Cable, *Fujikura Tehcnical Review*, Vol. 29, 57-62.

Tørum, A., Moghim, M.N., Westeng, K., Hidayati, N. and Arntsen, Ø. (2012), On berm breakwaters: Recession, crown wall wave forces, reliability, *Costal Eng*., Vol. 60, 299-318.

Woo, J., Na, W.B. and Yu, J.S. (2013), Analysis of the Falling Velocity of Underwater Anchor using Computational Fluid Dynamics, *Korean Association of Ocean Science and Technology Joint Workshop*, JeJu.

Zhang, X., Bai, J., Cao, G. and Chen, C. (2013), Optimizing HVDC control parameters in multi-infeed HVDC system based on electromagnetic transient analysis, *International Journal of Electrical Power & Energy Systems*, Vol. 49, 449-454.

Xiaohu Zhang, Jialin Bai, Guoyun Cao, Chen Chen

Zhu, Z., Mohanty, B. and Xie, H. (2007), Numerical investigation of blasting-induced crack initiation and propagation in rocks, *Int. J. Rock Mechanics & Mining Science*, Vol. 44, 412-424.